Electronic Supplementary Material (ESI) for Nanoscale.

Supporting information for

Metal-free highly-efficient photocatalyst for overall water splitting: C_3N_5 multilayer

Siyun Qi, Yingcai Fan, Junru Wang, Xiaohan Song, Weifeng Li, Mingwen Zhao*

School of Physics and State Key Laboratory of Crystal Materials, Shandong University, Jinan, Shandong, China

* Corresponding author, E-mail: zmw@sdu.edu.cn

1. The coordinates of a C_3N_5 unit cell in VASP POSCAR

C3N5

1.00000000000000

5.6463413344661335 0.0000000000000000 0.0000000000000000

-2.6349639679793042 6.1457086261608866 0.0000000000000000

0.0000000000000000 0.0000000000000000 20.0000000000000000

C N

5 8

Direct

0.4411575990945829 0.8535056704330239 0.2819406918712105

0.8382154311279963 0.8829561746136382 0.2628344335549135

0.5385888131353801 0.5396612590285671 0.2641510693639038

0.1597482880824560 0.5340850774184250 0.3254399608189339

0.2037592404463222 0.2299873977134275 0.2954473377038483

0.2212606537816646 0.8722625157316539 0.3091746268615189

0.6757702924202237 0.9891821661851289 0.2652805668901599

0.3888093334224679 0.6386310831906425 0.2913770470002716

0.0706606489768210 0.3139040646610639 0.3322328286926526

0.0881325370477426 0.9960151186469349 0.2861937643536638

0.4300219865274931 0.3220730365773293 0.2621631817327933

0.7750037046990311 0.6728914519012658 0.2449910131370164

0.0590614712377944 0.6750048528988958 0.3408234510191243

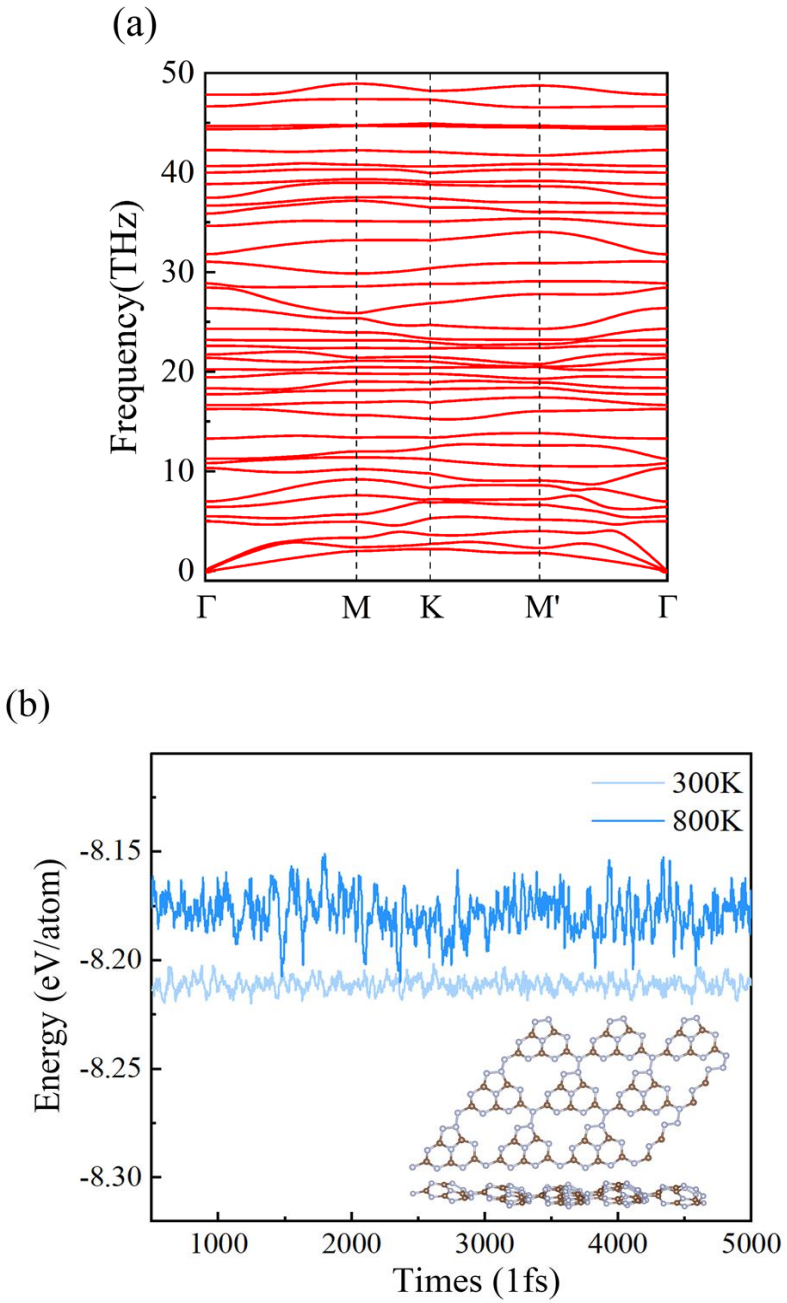

Fig. S1. (a) The phonon dispersion curves of C_3N_5 monolayer. (b) The energy fluctuations in molecular dynamics at 300 K and 800 K with the snapshots of C_3N_5 monolayer after a 5 ps simulation.

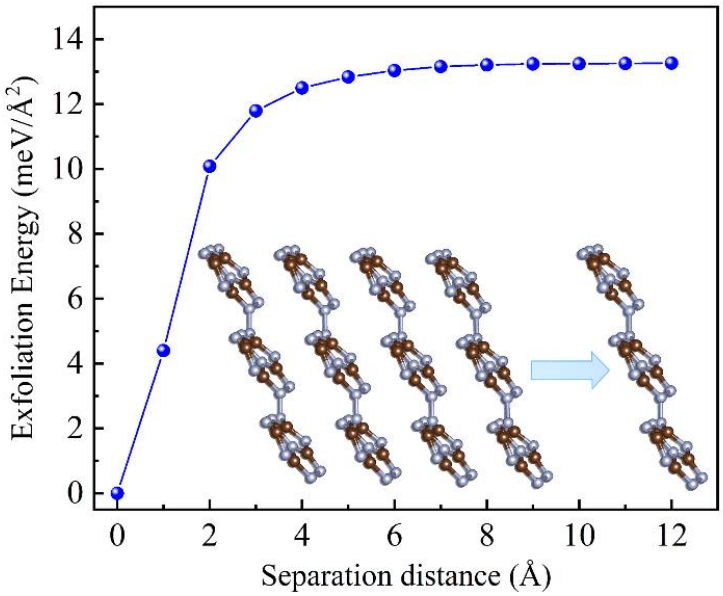

Fig. S2. Schematic diagram of monolayer exfoliation energy with the separation distance increasing in a five-layer slab model.

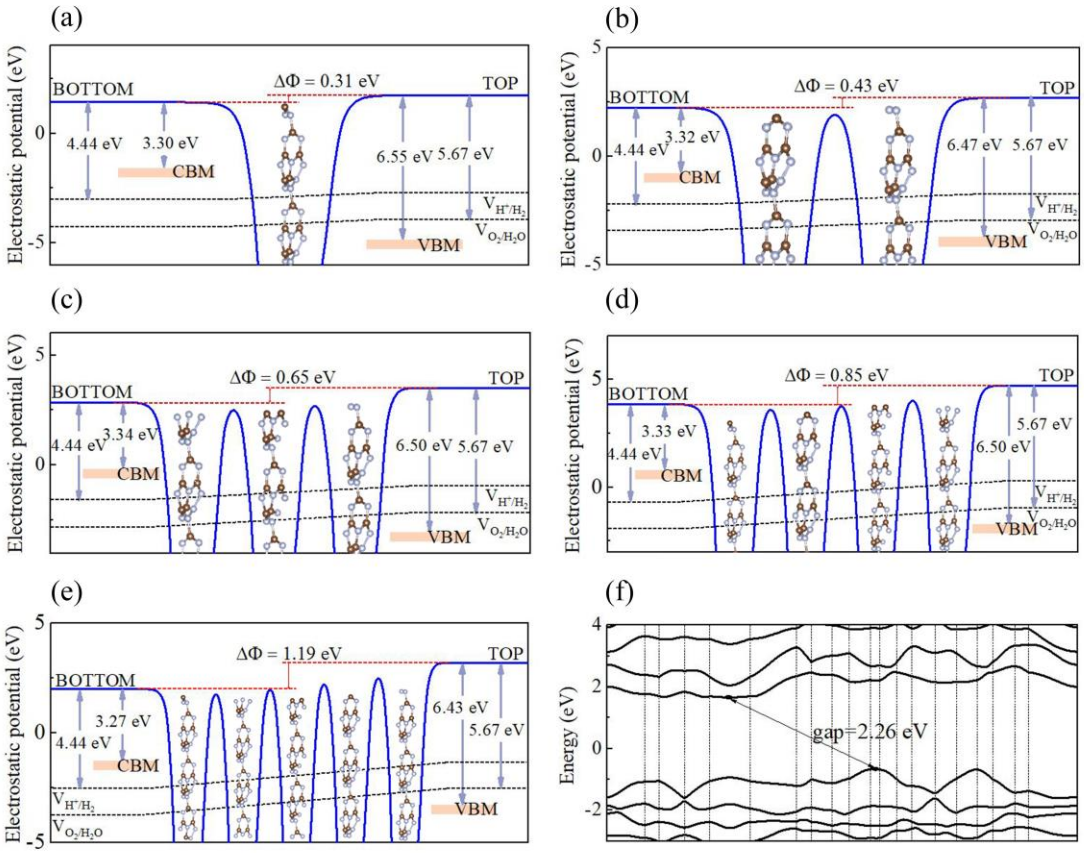

Fig. S3. The band edge position with respect to the water redox potential for (a) monolayer, (b) bilayer, (c) trilayer, (d) four-layers and (e)five-layers based on the HSE06 functional. (f) Band structure of the bulk C_3N_5.The vacuum level of the down surface is set to zero.

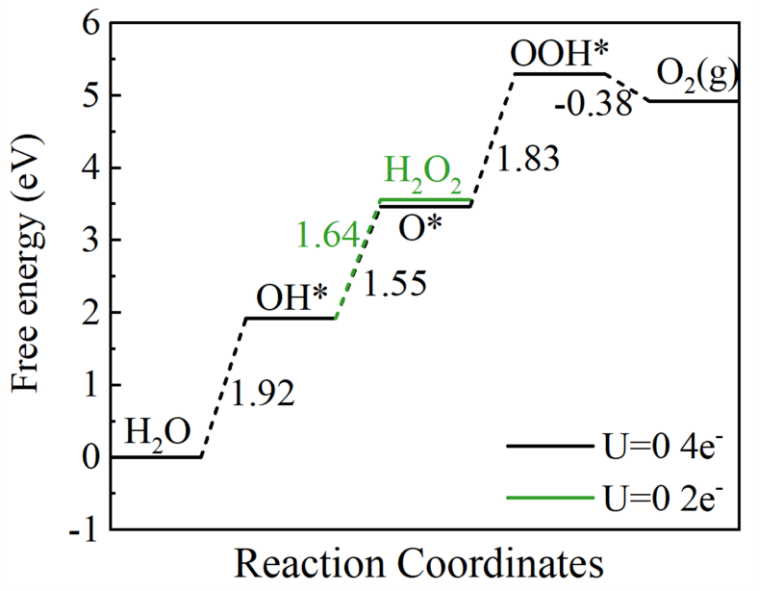

Fig. S4 Free energy diagrams for OER on C_3N_5 bilayer with $4e^-$ and $2e^-$ reactions.

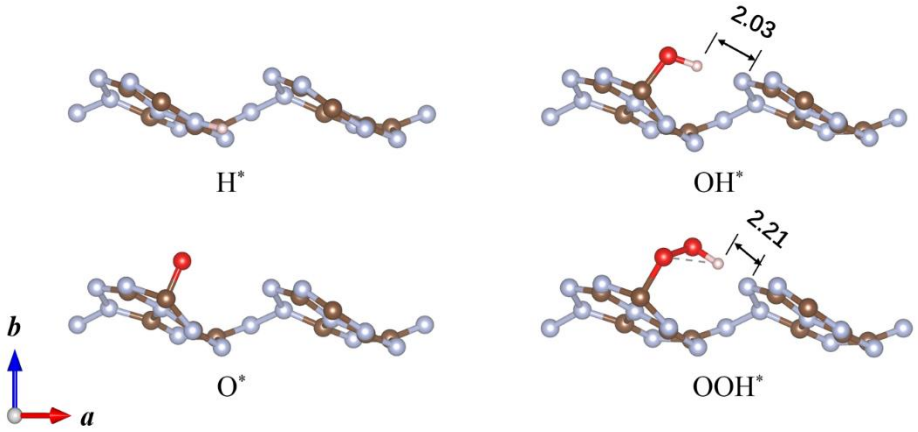

Fig. S5. Optimized geometries of the H*, OH* O* and OOH* intermediates in side views.

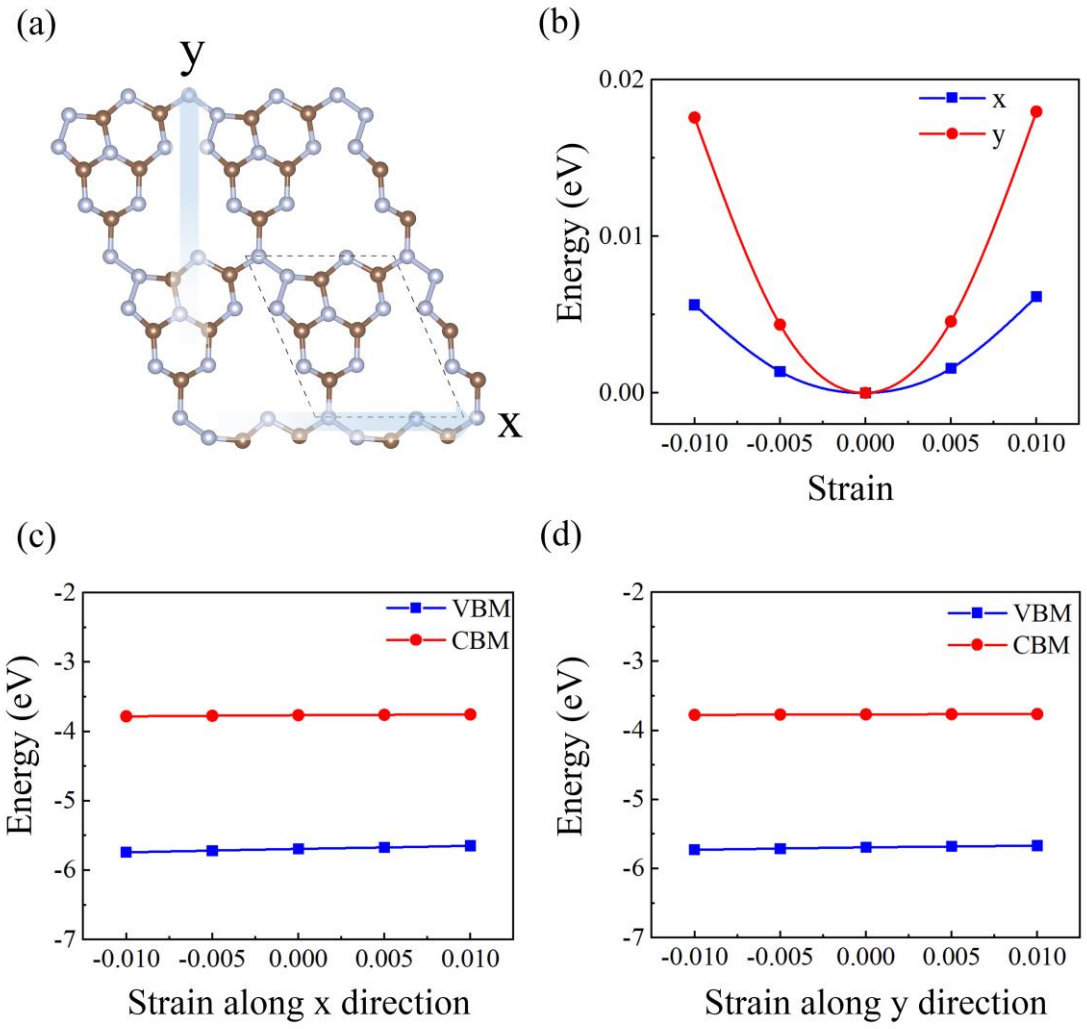

Fig. S6 (a) The selected directions of the carrier mobility of C_3N_5 monolayer. (b) The strain energy curves along the x- and y- directions for the monolayer. Band edge positions shifts of VBM and CBM in the (c) x and (d) y directions.

Table. S1. The zero-point vibration energy (E_{ZPE}) and the entropy correction value (TS) used in $\triangle G^*$ calculation, as well as the corresponding Gibbs free energy $\triangle G^*$ (eV) in monolayer (1L) and few-layered C_3N_5 (2L-5L).

species	E_{ZPE}	TS	$\triangle G_{1L}{}^*$	$\triangle G_{2L}{}^*$	$\triangle G_{3L}{}^*$	$\triangle G_{4L}{}^*$	$\triangle G_{5L}{}^*$
H_2	0.28	0.41	-6.91	-6.91	-6.91	-6.91	-6.91
H_2O	0.57	0.67	-14.32	-14.32	-14.32	-14.32	-14.32
OH^*	0.42	0	1.94	1.92	1.92	1.93	1.92
O^*	0.09	0	3.45	3.47	3.39	3.42	3.49
OOH^*	0.48	0	5.30	5.30	5.27	5.31	5.30
H^*	0.31	0	0.76	0.74	0.75	0.76	0.79